

# ADVANCED MATERIALS INTERFACES

---

Open Access

## Supporting Information

for *Adv. Mater. Interfaces*, DOI 10.1002/admi.202300955

Non-Oxidative Mechanism in Oxygen-Based Magneto-Ionics

*Tanvi Bhatnagar-Schöffmann, Patrick Schöffmann, Andrea Resta, Alessio Lamperti, Guillaume Bernard, András Kovács, Ludovic Largeau, Alan Durnez, Abdelmounaim Harouri, Xavier Lafosse, Djoudi Ourdani, Maria-Andromachi Syskaki, Yves Roussigné, Shimpei Ono, Rafal E. Dunin-Borkowski, Jürgen Langer, Dafné Ravelosona, Mohamed Belmeguenai, Aurelie Solignac and Liza Herrera Diez\**

## SUPPORTING INFORMATION

## Non-oxidative mechanism in oxygen-based magneto-ionics

Tanvi Bhatnagar-Schöffmann Patrick Schöffmann Andrea Resta Alessio Lamperti Guillaume Bernard András Kovács Ludovic Largeau Alan Durnez Abdelmounaim Harouri Xavier Laffosse Djoudi Ourdani Maria-Andromachi Syskaki Yves Roussigné Shimpei Ono R. E. Dunin-Borkowski Jürgen Langer Dafiné Ravelosona Mohamed Belmeguenai Aurelie Solignac Liza Herrera Diez

**Transmission electron microscopy (HR-TEM)**

The cross-sectional specimens for TEM measurements were prepared using focused Ga ion beam preparation following the conventional lift-out routine. The specimens then were studied using an electron probe aberration corrected transmission electron microscope (ThermoFisher Scientific Titan 80-200) operated at 200 kV. The scanning TEM images were processed and analysed using the Velox software. Fig.S1 (a) shows the presence of a highly disordered MgO layer in the as-grown state of the No-DL sample, whereas we observe a textured MgO layer in the as-grown DL sample as shown in fig. S1 (b). This observatoin strongly suggests that the dusting layer of Pt serves as a seed for the nucleation of crystalline grains in the MgO layer.

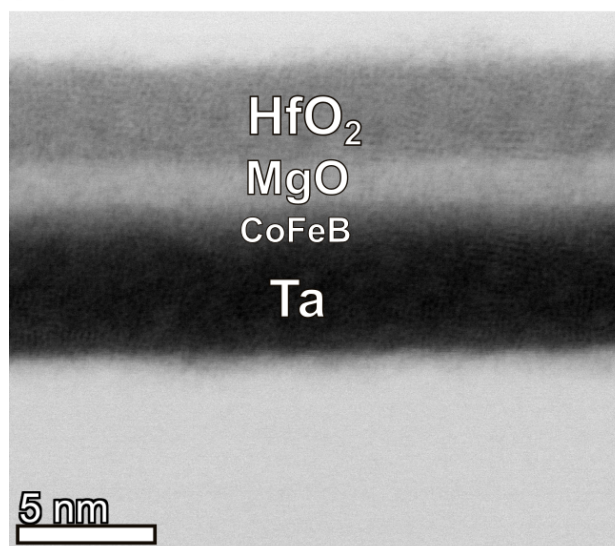
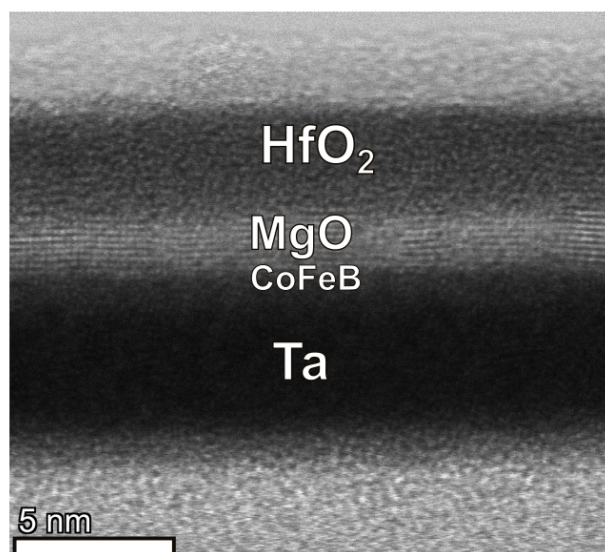
**(a) No-DL as-grown****(b) DL as-grown**

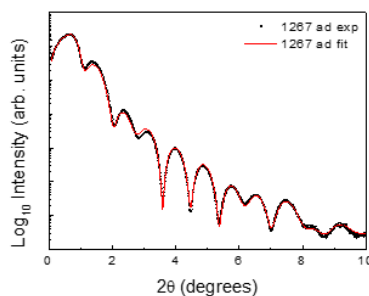
Figure S1: Bright-field scanning TEM images of (a) No-DL sample and (b) DL sample.

## X-ray reflectivity (XRR) measurements

XRR measurements have been conducted in a XRD3000 diffractometer (Italstructure), equipped with a long fine focus Cu  $K\alpha$  X-ray source ( $\lambda=0.154$  nm) monochromated by a parabolic mirror in w-2 $\theta$  configuration and using a scintillator point type detector. Data have been fitted using the MAUD software (L. Lutterotti, et al, Thin Solid Films 450, 34 (2004)). The MAUD software is freely available from the following link: <https://luttero.github.io/maud/>).

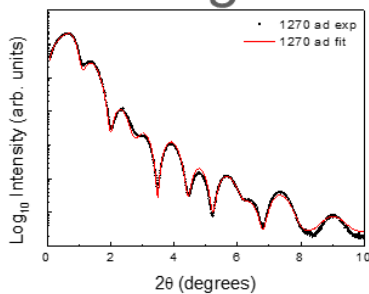
Fig. S2 shows XRR measurements and the corresponding fittings from where the thickness of the individual layers and the interface roughness have been obtained for the No-DL sample (a), as-grown DL sample and the DL sample after negative gate voltage application (-3.5V for 360s).

### a) No-DL



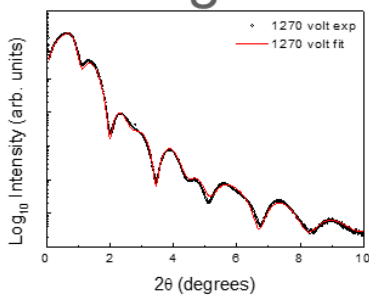
Layer	Thickness [nm]	Roughness [nm]
HfO <sub>2</sub>	3.089±0.004	0.3116±0.002
MgO	1.832±0.004	0.3117±0.003
CoFeB	0.640±0.007	0.1919±0.003
Ta	4.484±0.008	0.4948±0.004
SiO <sub>2</sub>	300	0.294±0.001
Si	-	0.150

### b) DL as-grown



Layer	Thickness [nm]	Roughness [nm]
HfO <sub>2</sub>	3.049±0.008	0.3656±0.003
MgO	1.812±0.007	0.3607±0.006
CoFeB	0.990±0.018	0.1229±0.005
Ta	4.349±0.019	0.6948±0.012
SiO <sub>2</sub>	300	0.2748±0.002
Si	-	0.150

### c) DL negative gate voltage



Layer	Thickness [nm]	Roughness [nm]
HfO <sub>2</sub>	3.180±0.011	0.5876±0.005
MgO	1.770±0.008	0.4239±0.005
CoFeB	0.866±0.014	0.1378±0.004
Ta	4.461±0.015	0.6761±0.010
SiO <sub>2</sub>	300	0.2921±0.002
Si	-	0.150

Figure S2: XRR measurements with fitting parameters for sample (a) No-DL sample and (b) DL samples in the as-grown state, as well as for (c) a DL sample after negative voltage gating (-3.5V for 360s).

## Vibrating sample magnetometry (VSM)

Fig. S3 (b) shows the magnetization as a function of the out of plane magnetic field for the DL sample in the as-grown state and after negative and positive gate voltage application. Fig. S3 (c) shows a zoom-in view in the low magnetic field region. In agreement with the anomalous Hall effect measurements presented in the main article, PMA increases after negative voltage application and it is significantly weakened after a subsequent positive gate voltage application. It is worth noting that the value of the saturation magnetisation does not present significant changes upon gating. The same effects are observed in the measurements conducted under an in-plane magnetic field (Fig. S3 (d) and (e)). The calculation of the saturation magnetisation was conducted considering the total sample area (10mm x 5mm) as well as the values of the layer thickness obtained from XRR measurements for the DL samples in the as-grown state and after negative voltage application. The thickness of the sample after positive voltage application is assumed to be the same as that after negative voltage application. These measurements were conducted on the same sample after subsequent applications of negative and positive gate voltages. Therefore, the consideration of a total area of 10mm x 5mm for the gated samples is an approximation, since about 20% of the sample area remained ungated, in order to leave space for the electrical connections. Despite this approximation, the value of the magnetic moment over area, or  $M * t$  as shown in Fig. S3 (a), does not present significant changes upon gating, which supports the idea of a non-oxidative magneto-ionic mechanism.

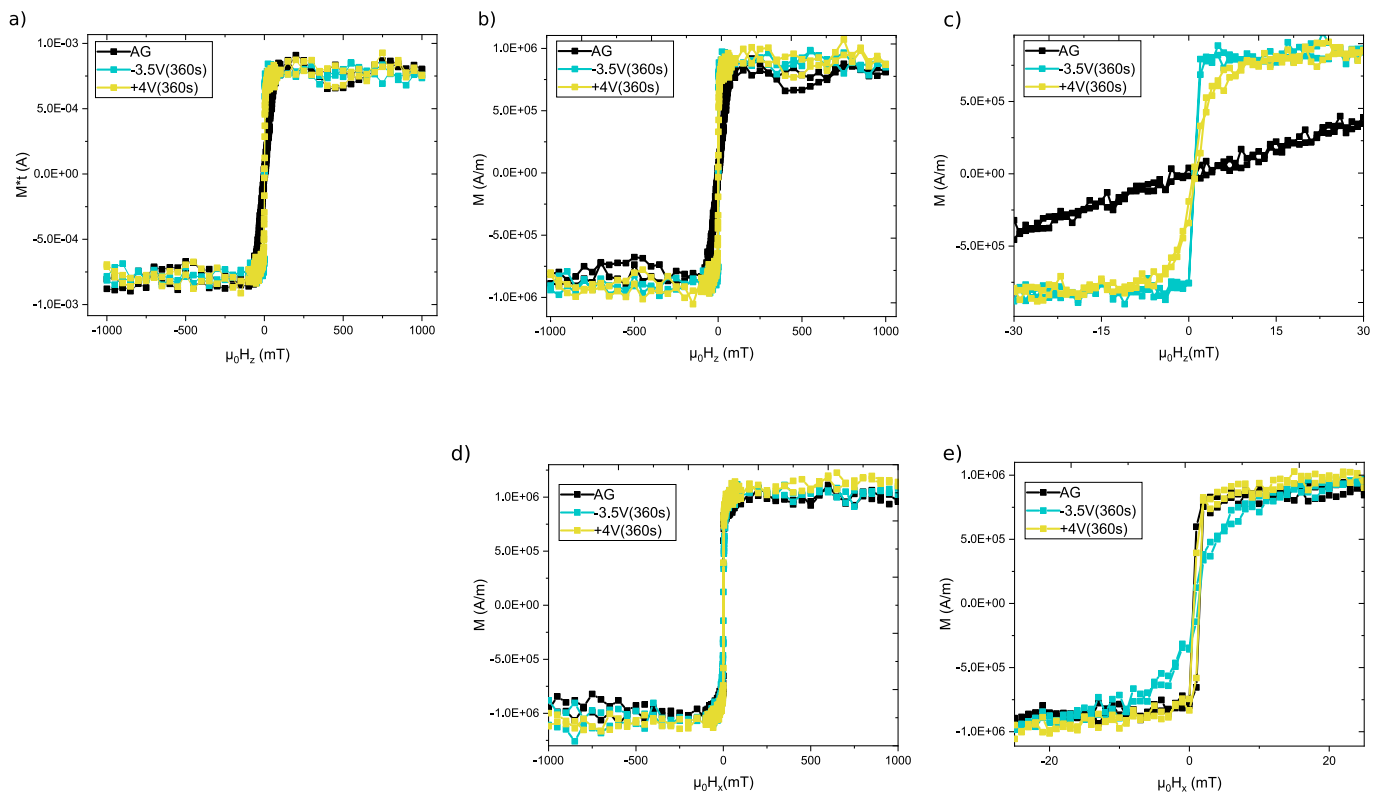


Figure S3: VSM measurements of (a) magnetic moment over area and (b) magnetisation, in the DL as-grown state and after positive and negative gate voltage application, as a function of a magnetic field applied out of plane. A zoomed-in view of (b) is presented in (c). Magnetization measurements under an in-plane magnetic field are presented in (d) and (e).

Fig. S4 shows (a) magnetic moment per unit area and (b) magnetization hysteresis loops for No-DL, DL and Pt-full sample measured under an out of plane (OOP) magnetic field. There is a progressive reduction of the magnetic moment per unit area going from the Pt-full sample to the DL sample and to the No-DL sample attributed to an increasing degree of oxidation at the CoFeB surface. Magnetization values were calculated using the layer thickness values of the No-DL sample and DL sample obtained from X-ray reflectivity, as presented above. In the case of the Pt-full sample, the thickness of the DL as-grown sample is assumed, which is very close to the nominal thickness of 1nm.

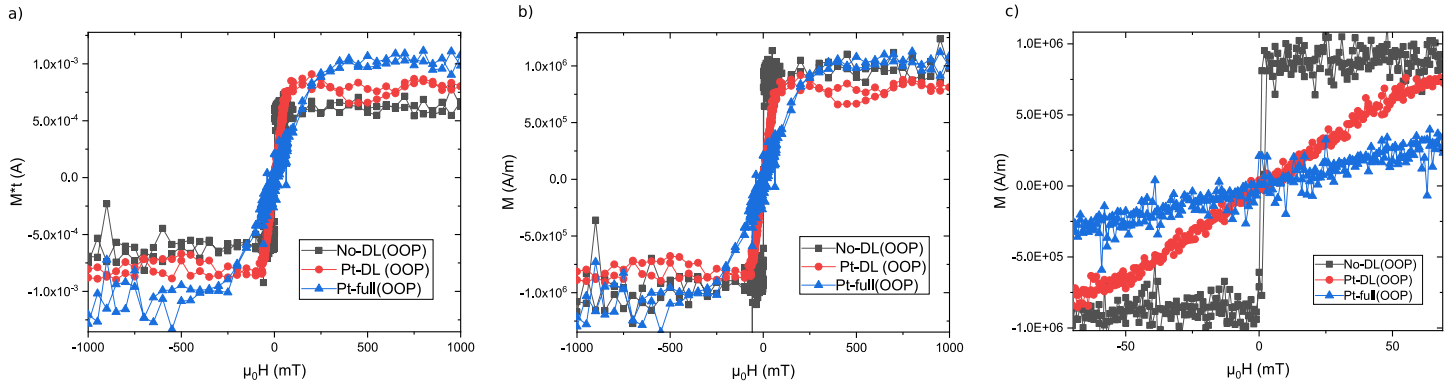


Figure S4: VSM measurements of (a) magnetic moment over area and (b) magnetisation of No-DL, DL and Pt-full samples with magnetic field applied along the out-of-plane direction. A zoomed-in view of (b) is presented in (c), showing that the sample No-DL exhibits PMA.

These measurements allowed for the calculation of the values of the saturation magnetisation  $M_s$  and the effective anisotropy  $K_{eff}$  for samples Pt-full, No-DL DL as-grown and DL after application of a negative gate voltage (DL-NV) which are presented in the table in Fig. S5.

Sample	$M_s$ OOP	Anisotropy field	$K_{eff}$
	A/m	T	J/m <sup>3</sup>
Pt full	1.03E+06	0.372	- 1.9158E+05
No-DL	9.9E+05	0.649	3.21255E+05
DL	8.32E+05	0.105	- 4.368E+04
DL-NV	8.91E+05	0.031	1.38105E+04

Figure S5: Table with values of  $M_s$  and the effective anisotropy  $K_{eff}$  for samples Pt-full, as-grown DL, No-DL and DL after application of a negative gate voltage (DL-NV).

## XAS: Oxygen K-edge fitting

Fig. S6 shows the model used to fit the oxygen K-edge spectrum obtained from XAS for the as-grown DL sample. This fitting was performed by using the reference data of the oxygen K-edge of MgO and HfO<sub>2</sub>. This fitting demonstrates that the XAS profile in the as-grown DL sample before voltage application is mainly dominated by the contributions from these two oxide layers.

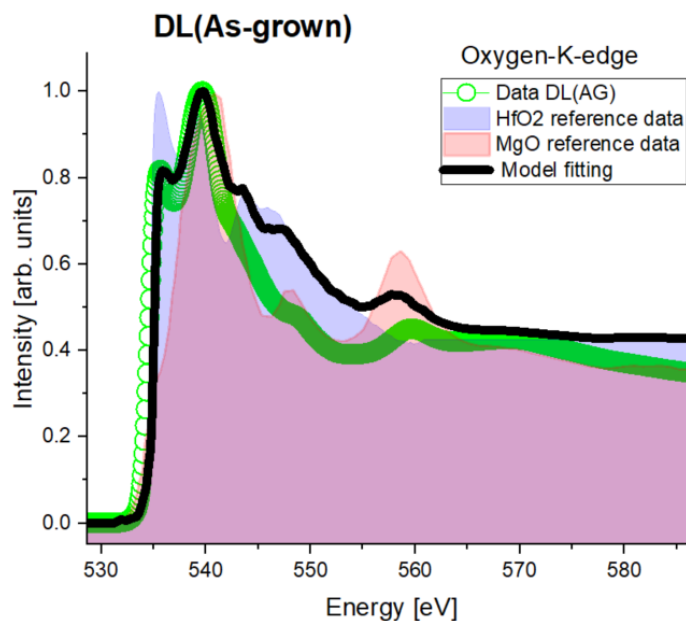


Figure S6: Model fitting of oxygen K-edge for the DL sample in its as-grown state.

## X-ray Diffraction (XRD) measurements

Fig. S7 shows the in-plane map of the DL sample after negative voltage application measured at CA. As indicated by the red arrow, around a  $\delta$  value of  $16.3\text{\AA}$  (for an energy of  $0.673\text{\AA}$ ), there is a strong but very localised signal. As the signal is very sharp, much more so than can be reasonably expected from the textured MgO film, and is not continuous for all angles of the sample rotation  $\omega$ , it is assumed that it comes from a source other than the film. Due to the proximity of this feature to the Mg(OH)<sub>2</sub> peak, that a  
ngle range was not taken into account for the interpretation of the data. However, the main peak of the Mg(OH)<sub>2</sub> in A does not seem to be significantly affected by the application of a positive gate voltage, as observed for peak B.

Fig. S8 shows that the sharp peak at feature A for  $-3.5\text{ V}$ , in LA is also an artifact similar to the case discussed for  $+4\text{ V}$ , CA. It is much less prominent, however, plotting only the high intensity regions reveals a similar non continuous signal not originating from the sample (marked (1)). On the other hand, the sharp peak corresponding to the Si(220) peak (marked (2)) is a result of an expected very sharp and intense substrate peak. The high intensity part is only a few pixels in size, so the peak can very easily appear very sharp.

+4V, CA

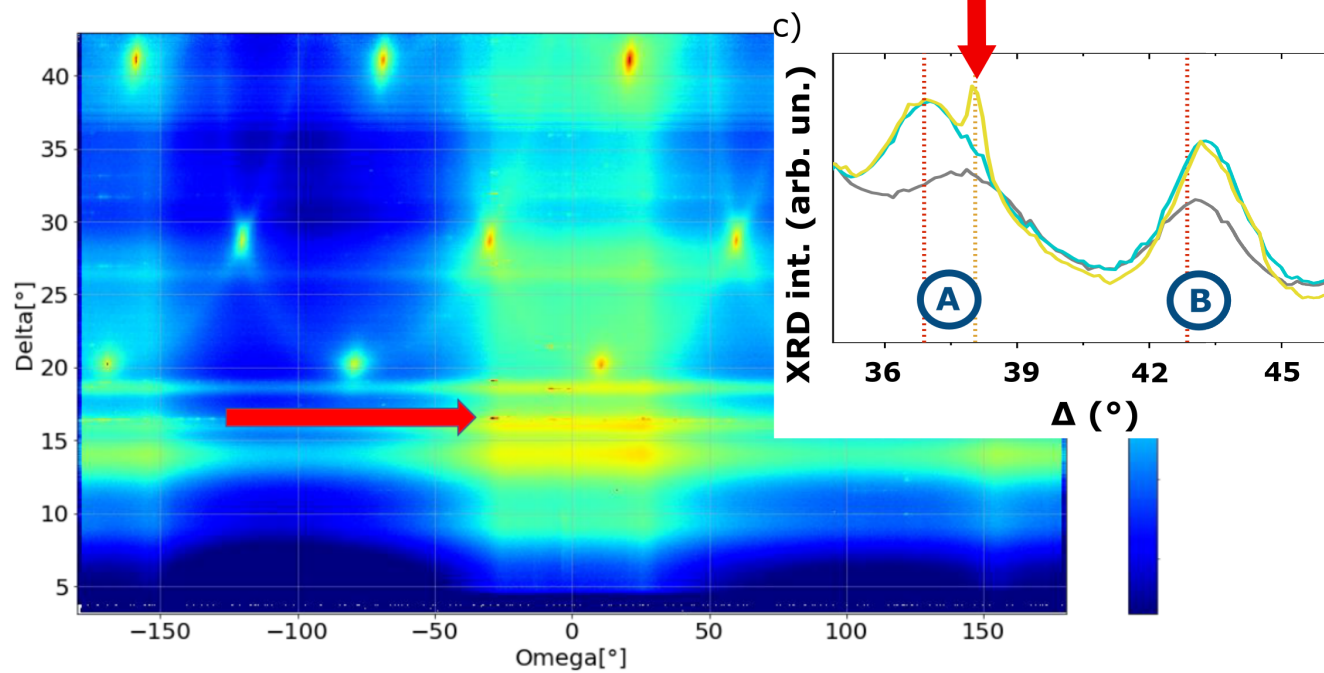


Figure S7: In-plane map of the DL sample gated with +4V recorded at Critical angle (CA).

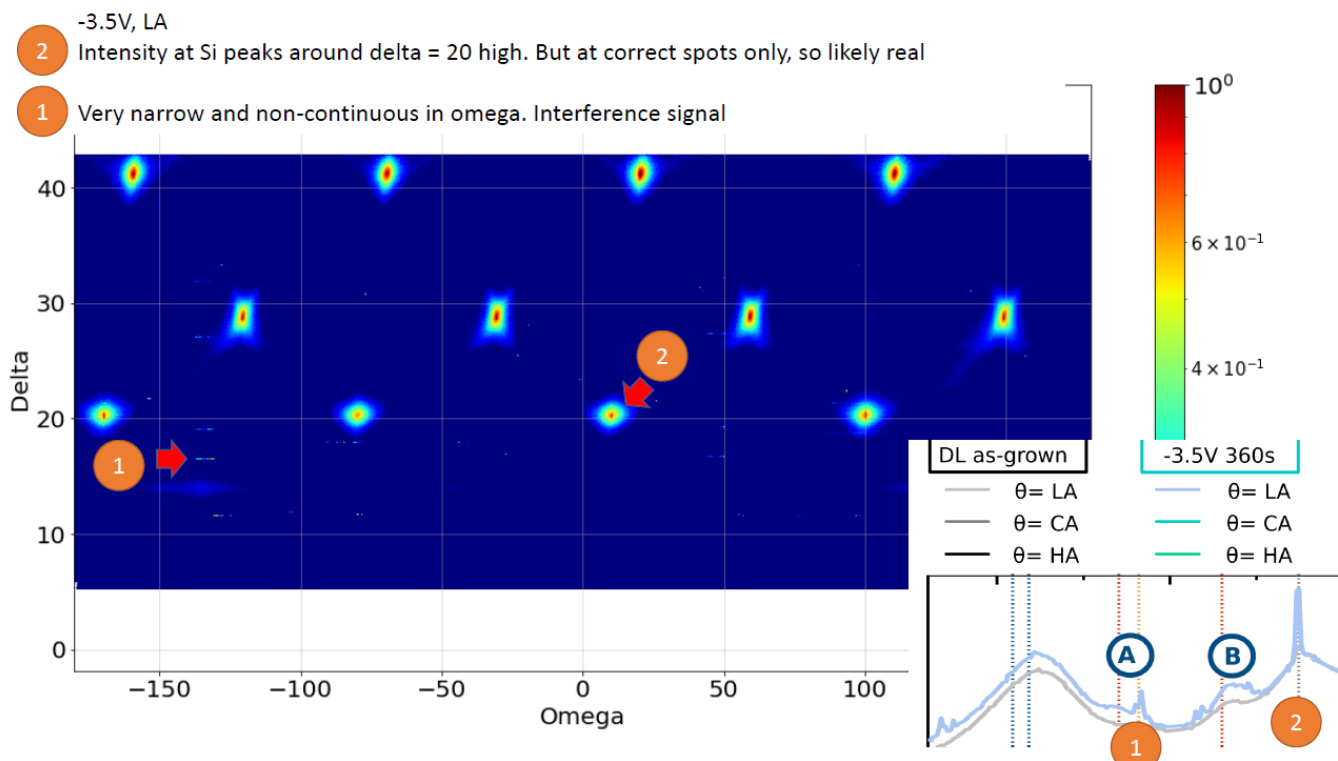


Figure S8: In-plane map of the DL sample gated with -3.5V recorded at low angle (LA).

## Additional anomalous Hall effect measurements (AHE)

The AHE measurements in the No-DL sample and its corresponding dependence on gate voltage have been reported in Ref. [5] (T. Bhatnagar-Schöffmann, et al. Appl. Phys. Lett. 2023, 122, 4 042402) of the main manuscript. For this sample, the initial state has PMA, and the gate voltage can only induce small modifications of the coercivity within the PMA regime. This is attributed to the relatively large component of the PMA in the as-grown sample, coming from the presence of a clean interface between CoFeB and MgO. In this context, the variation of the PMA induced by gating is not large enough to fully quench the PMA, and therefore a spin-reorientation transition is not observed.

In the case of the Pt-full layer, PMA is absent in the as-grown film and the gate voltages applied are not inducing any significant changes in the PMA component, as shown in Fig.S9. This is most likely due to the presence of a full 1nm thick layer separating the CoFeB from the interface with the MgO, giving the system a much stronger IPA anisotropy component.

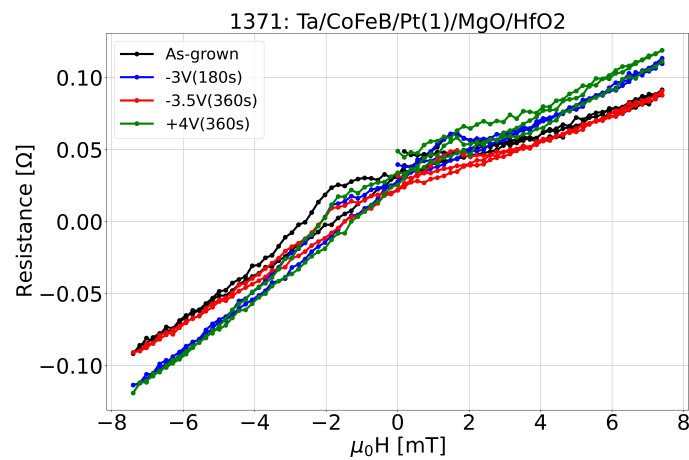


Figure S9: AHE measurements of the Pt-full sample in its as-grown state and after several gate voltage exposures using -3 V, -3.5 V and +4 V.